Early sedimentation and crossover kinetics in an off-critical phase-separating liquid mixture

J. Colombani* and J. Bert
Laboratoire Physique de la Matière Condensée et Nanostructures (UMR CNRS 5586), Université Claude Bernard Lyon 1, 6, Rue Ampère, F-69622 Villeurbanne Cedex, France
(Received 3 October 2003; published 27 January 2004)

Early sedimentation in a liquid mixture off-critically quenched in its miscibility gap was investigated with a light attenuation technique. The time evolution of the droplet distribution is characteristic of an emulsion coalescing by gravitational collisions. This sedimentation behavior gave access to the phase-separating kinetics, and a crossover on the way toward equilibrium was observed, which separates free growth from conserved order-parameter coarsening with a crossover time fitting well with theoretical predictions.

DOI: 10.1103/PhysRevE.69.011402 PACS number(s): 82.70.Kj, 64.75.+g, 64.60.My, 47.20.Bp

I. INTRODUCTION

The study of liquid-liquid phase separation constitutes a unique opportunity of observing the decay modes to equilibrium of a system abruptly brought into a metastable or nonequilibrium state. One benefits here from the universal behavior of the dynamical properties in the vicinity of a consolute critical point.

The leading quantity is the supersaturation Φ, corresponding to the equilibrium volume fraction of the minority phase. For values of Φ from $\frac{1}{2}$ to 0—or equivalently from deep to shallow quenches in the miscibility gap—the following stages can be encountered.

(1) For critical, i.e., quasisymmetric, quenches ($\Phi \simeq \frac{1}{2}$), the phase-separating mechanism is spinodal decomposition and has been abundantly investigated. Incipient domains from both phases grow from the most unstable wavelength of the concentration fluctuations ξ^- [1]. Afterward they coarsen by Brownian collision-induced coalescence, and the time evolution of their mean size scales as $t^{1/3}$ [2]. When they constitute a bicontinuous percolating medium, coarsening continues through surface-tension driven mechanisms (Rayleigh-like instability [3], coalescence-induced coalescence [4]) which induce a coarsening law linear with time [2].

(2) For off-critical, i.e., nonsymmetric, quenches, the phase-separating regime is nucleation and growth, where the nucleation has recently been stated as always being heterogeneous. This statement has been inferred from the monodispersity [5] and the undercriticality [6] of the nucleated droplet size. Growth proceeds through the diffusion of one of the components from the supersaturated background to a fixed number of growing nuclei (''free growth'') with a $t^{1/2}$ law [7]. After an intermediate regime where the volume fraction of minority phase reaches its equilibrium value Φ, two competing mechanisms are expected. First, when the solute-depleted layers around the growing droplets begin to interact, the coarsening mechanism may become Ostwald ripening, i.e., evaporation-condensation (undercritical nuclei dissipating into critical ones), obeying the $t^{1/3}$ Lifschitz-Slyozov (LS) law [8]. Along with this, as for the spinodal decomposition, when interfaces become sharp, coalescence may proceed through Brownian diffusion (BD) induced collisions of droplets, which also implies a $t^{1/3}$ law, with a different prefactor from the LS one [3]. The latter process should prevail at high Φ values and late times.

The volume fraction of minority phase Φ_T separating these two scenarios has been subject to much discussion but the latest reliable value should be $\phi_T \simeq 30\%$ [9]. Few results are available where Φ is systematically scanned between 0 and ϕ_T [9,10]. Hence some points remain questionable, among them the precise domain of existence of BD and LS coarsenings and the time of crossover between the free diffusion ($t^{1/2}$) and conserved order-parameter ($t^{1/3}$) regimes.

Whatever the regime, when the droplet size reaches a threshold value, gravity begins to prevail and sedimentation occurs. In the critical regime, two contributions to the study of sedimentation have to be mentioned. The first one identifies the successive stages during the prevailing of gravity [11]: macroscopic convection, sedimentation of droplets leading to a t^3 growth law, appearance of a meniscus sharing the mixture in two macroscopic phases, and residual sedimentation. The second one identifies the growth law during this residual sedimentation stage as $t^{0.27}$, as a consequence of coalescence by both sedimentation and Brownian diffusion [12]. In addition, sedimentation in the off-critical regime has never been systematically investigated and it is our aim to explore it.

Unexpectedly, this sedimentation study gives the opportunity to probe early times of the separation dynamics, difficult to access with light scattering methods, for instance [5]. Thereby we present here experimental evidence of a crossover on the way toward equilibrium of a phase-separating mixture.

II. EXPERIMENTS

For this purpose, we have chosen the water–isobutyric acid mixture, taking advantage of its room-temperature miscibility gap and the complete knowledge of its physicochemical properties.

Numerous experimental determinations of the phase diagram of this system may be found in the literature. To get a clear view of the experimental uncertainty (mentioned by Baumberger *et al.* [18]) on the coexistence curve, which is of

*Electronic address: Jean.Colombani@lpmcn.univ-lyon1.fr

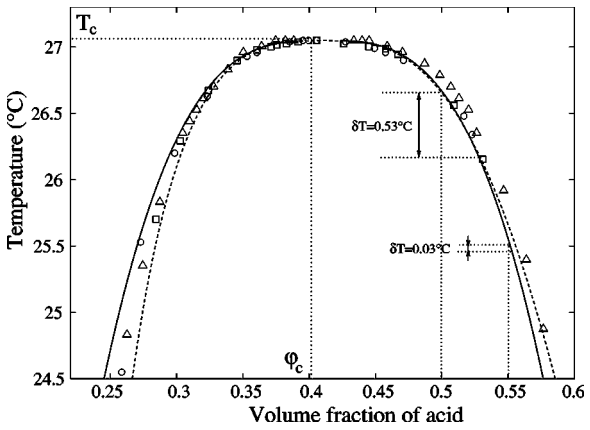

FIG. 1. Phase diagram (ϕ_{acid},T) of the isobutyric acid–water mixture from Woermann *et al.* [13] (○), Chu *et al.* [14] (□), Zhuang *et al.* [15] (△), Krall *et al.* [16] (dashed line), and Andrew *et al.* [17] (solid line). The critical temperatures have been matched to ours: $T_c = 27.05\,^{\circ}\mathrm{C}$. Our shallowest and deepest quenches are also represented.

great importance for computation of the volume fraction of the growing phase Φ, we gathered the most representative experimental phase diagrams on a single volume-fraction–temperature plot (cf. Fig. 1). The processing of the values of Hamano *et al.* [19] by Krall *et al.* [16] and the more recent interpretation of Greer's density measurements [20] by Andrew *et al.* [17] have been chosen rather than the corresponding original work. The acid mass fraction values c_{acid} of Krall *et al.* [16], Woermann *et al.* [13], Zhuang *et al.* [15], and Chu *et al.* [14] have been turned into volume fraction values ϕ_{acid} through $\phi_{acid} = (\rho_{phase}/\rho_{acid}) c_{acid}$, the densities ρ of the two phases and of isobutyric acid being taken from [20]. The critical temperature T_c shows a dispersion of more than one degree among the experiments, most certainly due to ionic impurities, which is of little consequence for the critical behavior [20,21]. So all curves have been adjusted to our experimental value $T_c = 27.05\,^{\circ}\mathrm{C}$. The data of Andrew *et al.* are quite recent and situated in the mean range of the other results [17]. Accordingly, their expression for the miscibility gap, $\Delta\phi_{acid} = \Delta\phi_0 \epsilon^{\beta}$ with $\Delta\phi_{acid} = \phi_{acid} - \phi_c$, $\phi_c = 0.4028$, $\Delta\phi_0 = 1.565$, $\beta = 0.326$, and $\epsilon = (T_c - T)/T_c$ the reduced temperature, has been chosen for our computation of Φ.

For the correlation length of the concentration fluctuations along the binodal line, the expression $\xi^- = \xi_0 \epsilon^{-\nu_\xi}$ with $\xi_0 = 1.8$ Å and $\nu_\xi = 0.63$ has been chosen [16]. The viscosities are $\eta = (\eta^B + A'\epsilon^{1/3})\epsilon^{-0.04}$ for the acid-rich phase and $\eta' = (\eta^B - A'\epsilon^{1/3})\epsilon^{-0.04}$ for the water-rich phase, with $\eta^B = 1.89$ mPl and $A' = 2.60$ mPl [16]. The diffusion coefficient of the mixture along the acid-rich branch of the coexistence curve is deduced from the above quantities using the Stokes-Einstein relation $D^- = k_B T/(6\pi\eta\xi^-)$.

To perform the quenches, an optical fused quartz cell containing the mixture is inserted inside a hollow copper block where a thermostat ensures water circulation, providing a temperature stabilization of the system within 0.01 K. The cell (optical path length 0.1 cm, 1 cm wide and 3 cm high) is illuminated by a laser beam and is observed by means of a charge-coupled device camera. For each concentration studied, the temperature of the coexistence curve has been visually determined (cloud point method) by a slow decrease of the temperature from the one-phase mixture (0.01 K temperature steps, each followed by a 20 min stabilization).

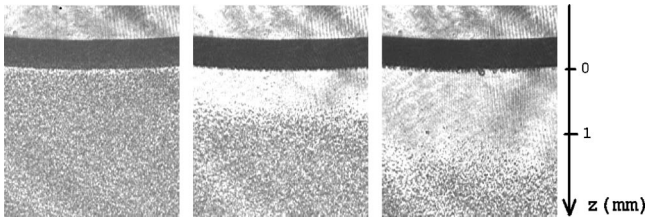

FIG. 2. Photographs of the sedimenting droplets in a mixture with $\phi_{acid} = 54\%$ for $\delta T = 0.13$ K, 3.5, 23.5, and 43.5 min after the quench.

Before each run, an energetic stirring is performed, followed by a 12 h annealing in the one-phase region 0.05 K above the coexistence curve. Then, the mixture is rapidly quenched through the binodal line ($\delta T = 0.03$–0.53 K below it), and this incursion into the miscibility gap leads to phase separation (cf. Fig. 2). In each case, the volume fraction of acid ϕ_{acid} (50–55 %) and the reduced temperature $\epsilon_f = (T_c - T_f)/T_c$ [$(2.3\text{–}6.4)\times 10^{-3}$ with T_f the absolute final temperature] are chosen in order to induce a volume fraction Φ of the growing phase between 0.3 and 10.5 %. The water-rich phase (density $\rho' \simeq 998\ \mathrm{kg\,m^{-3}}$) has been chosen as the nucleating and sedimenting phase to prevent wetting effects. Indeed, the isobutyric acid-rich phase (density $\rho \simeq 988\ \mathrm{kg\,m^{-3}}$) is known to preferentially wet the cell walls [17].

The evolution of the transmitted intensity along the vertical axis of the cell $I(z)$ is extracted from the video output—kept in its linear response domain—via image processing software (cf. Fig. 2). Averaging of $I(z)$ along a horizontal segment in the middle of the cell is carried out for each value of z to gain noise reduction. Then the light attenuation $I(z)/I_0$ is computed at several times during the phase separation. I_0 stands for the unscattered light intensity refracted by the homogeneous (droplet-free) mixture. This light attenuation is mainly due to scattering. The refractive indices of the two phases are very similar ($\Delta n \sim 10^{-2}$ in our ϵ range [17]), which is likely to induce low multiscattering. So in our Φ range and assuming a small polydispersity, the light attenuation $I(z)/I_0$ is linked at first order to the concentration of droplets $n(z)$ through the Lambert-Beer law $n(z) \sim -\ln[I(z)/I_0]$. Therefore the evolution of the $-\ln[I(z)/I_0]$ curves with time indicates the change of spatial distribution of droplets during sedimentation as displayed in Fig. 3.

Since the droplets are larger than the laser wavelength $\lambda = 0.532$ μm (see below), the attenuation should also be inversely proportional to their squared radius, which could have a slight influence on $-\ln(I/I_0)$. Therefore this expression constitutes a qualitative evaluation of n, but our analysis does not require a more precise determination, dealing only with abrupt slope changes in the behavior of n.

The time origin has been chosen as the cloud appearance

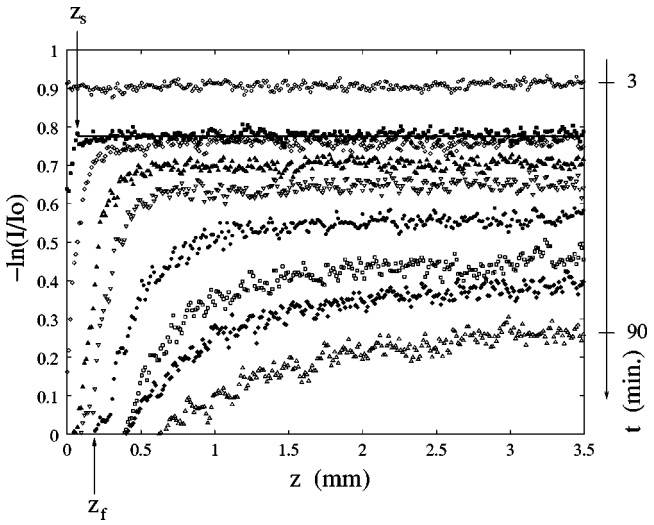

FIG. 3. Logarithm of the light attenuation $-\ln(I/I_0)$ across the cell as a function of the vertical position z and elapsed time t for a volume fraction of acid $\phi_{acid}=54\%$ and a quench depth $\delta T=0.37$ K.

time, and the space origin as the lower limit of the liquid-air meniscus (cf. Fig. 2).

Right after the quench, the cell becomes uniformly filled with erratically moving droplets forming an opalescent mist (horizontal upper line in Fig. 3). Then, in the vicinity of the meniscus the droplet concentration progressively decreases down to a zero value owing to an overall vertical motion of the droplets only visible at the top (clarification zone, droplet-free) and the bottom (sedimentation layer, not shown in Figs. 2 and 3) of the vessel. Afterward, the initial point z_f of the curves moves down and the value of the plateau sinks. The first feature reflects a expansion of the clarification zone and the second one is owing to the decrease of the bulk droplet concentration due to coalescence yielded by Brownian and/or gravitational collisions.

III. COARSENING MECHANISM DURING SEDIMENTATION

In order to highlight the respective roles of the Brownian and gravitational processes, knowledge of the Péclet number $\mathrm{Pe}=vR/D$ is needed (v is the mean sedimentation velocity, R the radius, and D the diffusion coefficient of the droplets). Indeed, this number compares the mean sedimentation velocity v to the Brownian velocity D/R.

With this purpose, we turn to the clarification zone behavior. Its expansion can be followed in Fig. 3 through the increase with time of the intercept z_f of the light attenuation curve with the abscissa axis. In other words, z_f corresponds to the upper limit of the sedimentation front. At this point, the droplets are very scarce, so they can be considered as evolving in a quasi-infinitely dilute regime. Therefore the sedimentation-induced convective part of their motion is insignificant [22], and their velocity v_f corresponds to the stationary velocity of isolated droplets of radius R_f, given by the Hadamard formula [23]:

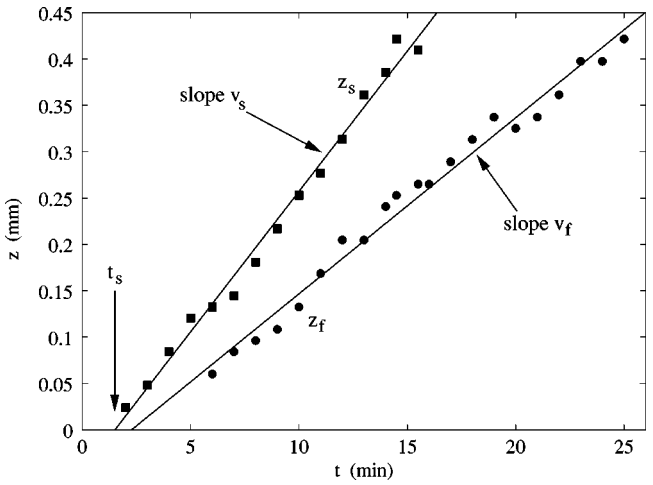

FIG. 4. Position of the beginning point z_f and of the start of the plateau z_s of the light attenuation curves as a function of time in the ($\phi_{acid}=52\%, \delta T=0.12$ K) case. The lines are least-squares fits of the values. The t_s time is also shown.

$$v_f=\frac{2(\eta'+\eta)(\rho'-\rho)R_f^2 g}{3(3\eta'+2\eta)\eta} \tag{1}$$

with g the gravitational acceleration, η' and η, respectively, the viscosity of the water-rich drop and of the acid-rich surrounding fluid, and ρ' and ρ their respective densities. To assess the validity of this expression, two checks have been carried out. This formula is valid provided that inertia effects are negligible. This requirement is guaranteed by a low Reynolds number $\mathrm{Re}=R_f v_f \rho/\eta$, always smaller than 2×10^{-6} in our case. Second, even if long-range interdroplet hydrodynamic interactions induced an average settling velocity v_{av} lower than the Hadamard velocity v_f, the hindered settling function $f(c)=v_{av}/v_f$ would take values between $\frac{1}{2}$ and 1 for Φ ranging from 1 to 10% [22]. So these interactions would not yield a noticeable change of the value of the settling velocity.

As v_f is given by the slope of the $z_f(t)$ line (cf. Fig. 4), the droplet radius R_f at the appearance of the clarification zone can be computed from Eq. (1). R_f ranges between 3.3 and 8.9 μm. Knowing that the diffusivity of spherical droplets immersed in a liquid of viscosity η is $D_f=k_BT/(5\pi\eta R_f)$,[1] their Péclet number $\mathrm{Pe}_f=v_f R_f/D_f$ can be computed:

$$\mathrm{Pe}_f=\frac{15\pi\eta^2(3\eta'+2\eta)v_f^2}{2k_BT(\eta'+\eta)(\rho'-\rho)g}. \tag{2}$$

[1]This expression is obtained by writing, in the Einstein expression of the diffusivity of one droplet $D=k_BT/\mu$, the mobility μ as v_f/F_g with v_f the Hadamard sedimentation velocity of Eq. (1) taken with $\eta=\eta'$ and $F_g=(\rho'-\rho)g(4/3)\pi R_f^3$ the gravitational force exerted on the droplet.

Pe_f is found to range between 8 ($\phi_{acid}=50\%$ and $\delta T=0.53\,^{\circ}\mathrm{C}$) and 371 ($\phi_{acid}=53\%$ and $\delta T=0.13\,^{\circ}\mathrm{C}$). Recalling that these droplets experience almost no coalescence owing to their dilute environment, their growth is the slowest of the vessel, their radius is the smallest, and their velocity is minimal among all droplets, so we can argue that $\mathrm{Pe}\gg 1$ in the bulk sedimenting liquid. Therefore gravitation-induced hydrodynamic interactions should prevail over Brownian diffusion as the coalescence mechanism.

To confirm this statement, we consider theoretical studies of the coalescence of non-Brownian sedimenting polydisperse droplets immersed in an immiscible fluid [24]. The evolution of the volume fraction of droplets with position in the vessel at different times (Fig. 7 of Ref. [24]) shows a strong similarity with our light attenuation curves of Fig. 3. Therefore the droplet density in our sedimenting mixture displays the same evolution as predicted for non-Brownian droplets and, at variance with some predictions [12,18], the driving force of coalescence is likely to consist only of gravitational collisions.

IV. PHASE SEPARATION DYNAMICS

What can we learn now about the drop growth law during this stage of phase separation? To address this point, we focus on the early appearance of sedimentation. When growing droplets experience a gravitational force overwhelming Brownian diffusion, the symmetry of their displacement is broken and they exhibit an average descending motion. This incipient settling motion can be traced in Fig. 3 through the displacement with time of the beginning z_s of the curve plateau. In other words, we follow with z_s the initial mean trajectory of the droplets settling from the meniscus. We concentrate on early times, where the intercept of the rising curve and the plateau is unambiguous. If the Péclet number Pe_s, mean sedimentation velocity v_s, and diffusivity D_s of these settling droplets are known independently, their radius can be computed, considering the definition of Pe_s, via $R_s=\mathrm{Pe}_s D_s/v_s$. Using the above-mentioned Einstein expression for D_s, one gets $R_s=\sqrt{\mathrm{Pe}_s k_B T/(5\pi\eta v_s)}$.

The value of η is given above and v_s is accessible through the slope of the $z_s(t)$ line (cf. Fig. 4). So at this point we need a determination of the only missing value Pe_s to be able to calculate R_s at least at one particular time of the coarsening.

The sedimentation regime is entered when the Péclet number sufficiently exceeds unity. We will tentatively consider that this is the case when the sedimentation velocity becomes one order of magnitude larger than the diffusive velocity. The time t_s of this start of sedimentation is measured in extrapolating the $z_s(t)$ curve to zero. $z_s(t)$ has been seen to remain linear at early times, which enables a well-defined extrapolation of t_s (cf. Fig. 4). So at t_s we assume that $\mathrm{Pe}_s=10$ and R_s can be computed with the above-mentioned formula. As expected for droplets at the nonsedimenting-sedimenting transition, R_s ranges between 1.0 and 3.2 μm for our quenches.

Therefore we use our knowledge of the sedimentation behavior as a probe to determine the droplet radius R_s just when sedimentation sets in. Accordingly, the R_s values of the different quenches are characteristic of the early coarsening mechanisms preceding sedimentation (free growth, BD, LS) and not related to the settling behavior itself.

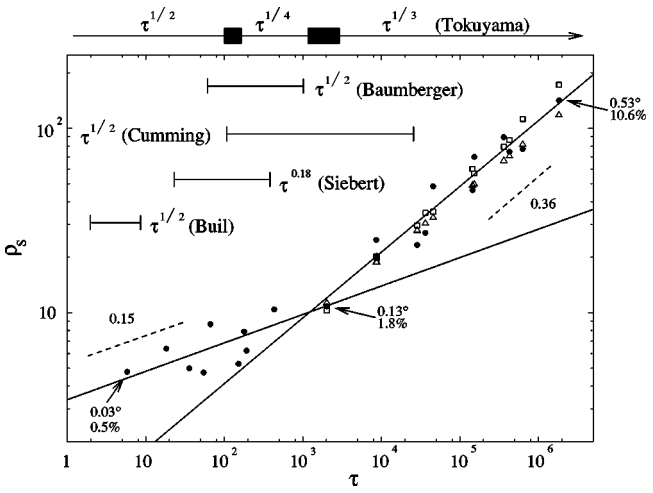

FIG. 5. Evolution with reduced time τ of the reduced droplet size ρ_s at the end of the nonsedimenting regime (black dots). The open triangles and squares are, respectively, the theoretical values of ρ_s for an Ostwald ripening and a Brownian diffusion-coalescence growth. It should be noticed that each point corresponds to one experiment. Ranges of growth exponents available in the literature for $\Phi<10\%$ have also been added (references given in the text). The quench depth δT and the volume fraction of the growing phase Φ are mentioned for some representative points.

Concerning the choice of Pe_s, Wang and Davis performed computations in an immiscible mixture experiencing simultaneous Brownian and gravitational collisions [25]. Using their predictions, we computed the mean radius R_s of the coalescing droplets after a time estimated as t_s in the most unfavorable case of viscosity, dispersity, and settling velocity. We find that $R_s\simeq 1.5R_0$ (R_0 is the initial radius) for an initial Péclet number $\mathrm{Pe}_s=1$ and $R_s\simeq 2.4R_0$ for $\mathrm{Pe}_s=10$. Therefore we can conclude that (1) whatever the choice of Pe_s, gravity has not significantly modified the coarsening dynamics after an elapsed time t_s and (2) this minor influence on R_s, if any, is comparable for Pe_s ranging from 1 to 10. Furthermore, $R_s\sim\sqrt{\mathrm{Pe}_s}$, which induces a weak influence of the choice of Pe_s, between 1 and 10, on the computation of R_s.

To allow comparison between the dynamics of all experiments, we put the time and radius values in a dimensionless form: $\tau=t/t_c$ and $\rho=R/R_c$. The renormalization quantities are the radius of an initial critical nucleus $R_c=\alpha/\Phi$ and the relaxation time of this nucleus $t_c=\alpha^2/\Phi^3 D^-$, with α a capillary length estimated as $\alpha=\xi^-/3$ [7].

We now dispose of one point (τ_s,ρ_s) for each experiment, covering five decades of reduced time. Figure 5 displays the evolution of ρ_s as a function of τ_s. We first ascertain that all experiments merge onto a single curve, whatever the initial supersaturation. The second striking feature lies in the presence of a crossover between two coarsening stages. The first behavior can tentatively be fitted by a power law of

exponent $\simeq 0.15$. Such a slow radius evolution is expected at the end of the free growth regime and reflects the overlapping of the solute-depleted shells around the nuclei [26]. The second behavior displays a growth exponent $0.36 \simeq \frac{1}{3}$, which is the well-known exponent of interface-reduction coarsenings (LS and BD). To our knowledge this constitutes the first experimental observation of the crossover between free growth and constant volume-fraction coarsening in a liquid system. This crossover takes place at $\tau_{CO} \simeq 1 \times 10^3$.

The experimental and theoretical growth laws available for $\Phi < 10\%$ in the literature have also been added in Fig. 5. Surprisingly, no other measurements exist in the $t^{1/3}$ range for $\Phi < 10\%$ except those of Wong and Knobler, which seem to display a progressive change of slope and are therefore delicate to deal with [2], and those of White and Wiltzius, the dimensionless parameters of which are not available [27]. Concerning the end of free diffusion, our growth exponent is equivalent to Siebert and Knobler's (0.18) [28] and is compatible with the theoretical prediction of Tokuyama and Enomoto ($\frac{1}{4}$) [26]. The validity domain of this intermediate stage is also compatible with the $t^{1/2}$ range of Buil *et al.* [6] but is not consistent with those of Baumberger *et al.* [18] and Cumming *et al.* [5]. The latter dealt with polymer blends and this could account for the dynamics discrepancy or at least for the difficulty of computing equivalent dimensionless quantities in simple (acid/water) and complex (polymer blends) fluids. The inconsistency with the former remains unexplained. The crossover time compares well with Tokuyama and Enomoto's theoretical value $1.1 \times 10^3 < \tau_{CO}^{theo} < 2.8 \times 10^3$, the lower value computed at $\Phi = 1\%$ and the upper one at $\Phi = 10\%$ [26].

As the exact mechanism of the late decompositional stage still remains debatable [27], we have drawn in Fig. 5 the theoretical values of $\rho_s(\tau)$ predicted by the Lifschitz-Slyozov and Brownian diffusion coarsening laws, computed without adjustable parameters. Written in reduced units, the expressions are $\rho_s = [1 + (4/9) f(\Phi) \tau]^{1/3}$ [$f(\Phi)$ being a numerically estimated function] for evaporation-condensation [8] and $\rho_s = \{144 \Phi \tau / [\ln(0.55 R_s/\delta)]\}^{1/3}$ (with $\delta \simeq \xi^-$) for Brownian diffusion coalescence [3]. Unfortunately, although experimental and theoretical values superimpose,[2] the dispersion of our values is too large to discriminate between the LS and BD laws, and their closeness banishes any hope of doing so from $\rho(\tau)$ curves.

V. CONCLUSION

We have determined the leading coarsening mechanism (gravitational collisions) during the sedimentation regime in a homogeneous mixture plunged into a metastable state. In addition, thanks to the superposition of numerous sedimentation experiments in such systems, the universal crossover time between free growth and ripening by diffusion of a conserved order parameter has been measured and agrees with theoretical predictions. Unfortunately, the nature of the second mechanism has not been settled and the existence range of Ostwald ripening and Brownian coalescence coarsening remains to be established. Finally, experimental access to the complete scenario of off-critical coarsening from the $t^{1/2}$ to the $t^{1/3}$ law would bring a comprehensive view of the phase-separation process and a complete verification of the nucleation and growth theory.

ACKNOWLEDGMENTS

We acknowledge CNES (French space agency) for financial support, Bénédicte Hervé, Laurence Heinrich, and Richard Cohen for experimental help, and Jean-Pierre Delville, Régis Wunenburger, Christophe Ybert, and Elisabeth Charlaix for fruitful discussions.

[2]This superimposition justifies *a posteriori* our $\mathrm{Pe}_s = 10$ choice for the computation of ρ_s. Nevertheless, a change in Pe_s would have implied only a vertical translation of the values but would have had no influence on the kinetics and crossover time.

[1] J. Cahn, Trans. Metall. Soc. AIME **242**, 166 (1968).
[2] N. Wong and C. Knobler, Phys. Rev. A **24**, 3205 (1981).
[3] E. Siggia, Phys. Rev. A **20**, 595 (1979).
[4] V. Nikolayev, D. Beysens, and P. Guénoun, Phys. Rev. Lett. **76**, 3144 (1996).
[5] A. Cumming, P. Wiltzius, F. Bates, and J. Rosedale, Phys. Rev. A **45**, 885 (1992).
[6] S. Buil, J. Delville, and A. Ducasse, Phys. Rev. Lett. **82**, 1895 (1999).
[7] J. Langer and A. Schwartz, Phys. Rev. A **21**, 948 (1980).
[8] N. Akaiwa and P. Voorhees, Phys. Rev. E **49**, 3860 (1994).
[9] F. Perrot, D. Beysens, Y. Garrabos, T. Fröhlich, P. Guenoun, M. Bonetti, and P. Bravais, Phys. Rev. E **59**, 3079 (1999).
[10] I. Hopkinson and M. Myatt, Macromolecules **35**, 5153 (2002).
[11] C. Chan and W. Goldburg, Phys. Rev. Lett. **58**, 674 (1987).
[12] F. Cau and S. Lacelle, Phys. Rev. E **47**, 1429 (1993).
[13] D. Woermann and W. Sarholz, Ber. Bunsenges. Phys. Chem. **69**, 319 (1965).
[14] B. Chu, F. Schoenes, and W. Kao, J. Am. Chem. Soc. **90**, 3042 (1968).
[15] Z. Zhuang, A. Casielles, and D. Cannell, Phys. Rev. Lett. **77**, 2969 (1996).
[16] A. Krall, J. Sengers, and K. Hamano, Phys. Rev. E **48**, 357 (1993).
[17] W. Andrew, T. Khoo, and D. Jacobs, J. Chem. Phys. **85**, 3985 (1986).
[18] T. Baumberger, F. Perrot, and D. Beysens, Phys. Rev. A **46**, 7636 (1992).
[19] K. Hamano, S. Teshigawara, T. Koyama, and N. Kuwahara, Phys. Rev. A **33**, 485 (1986).
[20] S. Greer, Phys. Rev. A **14**, 1770 (1976).
[21] R. Cohn and D. Jacobs, J. Chem. Phys. **80**, 856 (1984).
[22] R. Davis and A. Acrivos, Annu. Rev. Fluid Mech. **17**, 91 (1985).

[23] J. Hadamard, C. R. Hebd. Seances Acad. Sci. **152**, 1735 (1911).
[24] H. Wang and R. Davis, J. Fluid Mech. **295**, 247 (1995).
[25] H. Wang and R. Davis, J. Colloid Interface Sci. **178**, 47 (1996).
[26] M. Tokuyama and Y. Enomoto, Phys. Rev. Lett. **69**, 312 (1992).
[27] W. White and P. Wiltzius, Phys. Rev. Lett. **75**, 3012 (1995).
[28] E. Siebert and C. Knobler, Phys. Rev. Lett. **54**, 819 (1985).